

COMPARATIVE ANALYSIS OF QUANTITATIVE INDICES FOR EVALUATING THE LIQUEFACTION POTENTIAL OF MEDIUM-DENSE COHESIONLESS SOIL

Ali Zakariya^{1*}, Ahmad Rifaí², and Sito Ismanti³

ABSTRACT

Earthquakes that induced liquefaction have occurred in several regions in Indonesia, including Bantul Regency during the 2006 Bantul earthquake. The study location is the Kretek 2 Bridge in the Opak River Estuary, Bantul Regency, Yogyakarta Special Region Province. This area features medium-dense sandy soil with a high liquefaction potential. This study estimated the safety factors related to liquefaction using a simplified procedure. In addition, this study analyzed the quantitative index of liquefaction potentials using the Liquefaction Potential Index (LPI), Liquefaction Reduction Number (LRN), Liquefaction Risk Index (LRI), Liquefaction Severity Index (LSI), Liquefaction Displacement Index (LDI), and Post-liquefaction Settlement approaches. The results showed that liquefaction occurred predominantly at a depth of 1.5-6 m. For the LPI and LRN, the soil was classified as “very low” to “high” and “low” to “very high” for liquefaction potential, respectively. While the LRI result was in the “low” to “medium” risk categories, the LSI output was in the “non-liquefied” to “low” severity classification. The LDI and post-liquefaction settlement calculated by 1-D reconsolidation were 3.9 m and 0.12 m, respectively. Each method has different results; the LPI and LRN are more inclined to the possibility of a liquefaction event occurring, while the LRI and LSI emphasize the level of risk and severity of liquefaction damage. Furthermore, the LDI and post-liquefaction settlement are indicators of area damage measured in meters horizontally and vertically if liquefaction occurs.

Key words: liquefaction potential, medium-dense sandy soil, safety factor, simplified procedure, quantitative index.

1. INTRODUCTION

With many faults and tectonic subduction, Indonesia is often hit by earthquakes that can induce liquefaction. On May 27th, 2006, liquefaction occurred after a strong earthquake that struck Bantul with a moment magnitude (Mw) of 6.2 and a focal depth of 17.1 km (Supartoyo *et al.* 2014). Buana and Agung (2015) reported that liquefaction occurred after the 2006 Bantul earthquake (see Fig. 1). This event was categorized as a shallow earthquake in the Opak fault zone with a hypocentral depth of approximately 10-20 km (Nurbaiti *et al.* 2019). Wibowo and Sembri (2017) also studied the Opak fault with seismicity analysis based on earthquake events that occurring during 2008 to 2017 and concluded that the hypocenters of these earthquakes were located at depths of approximately 10-20 km. Referring to the geologic map of the Yogyakarta Special Region, the southern Bantul area has young volcanic deposits related to Mount Merapi and widespread alluvial deposits (Rahardjo *et al.* 1977). As stated by Youd and Perkins (1978), the coastal area with young Quaternary sediment and shallow groundwater features a high liquefaction potential. Thus, the Yogyakarta Special Region, which is near a fault, is at high risk of strong earthquakes and soil liquefaction.

Manuscript received November 19, 2022; revised May 22, 2023; accepted May 24, 2023.

¹*M.Eng. Graduate (corresponding author), Department of Civil and Environmental Engineering, Universitas Gadjah Mada, Indonesia and Directorate of Bridge Construction, Directorate General of Highways, Ministry of Public Works and Housing, Jakarta, Indonesia (e-mail: alizakariyast@mail.ugm.ac.id).

²Associate Professor, Department of Civil and Environmental Engineering, Universitas Gadjah Mada, Indonesia.

³Ph.D., Department of Civil and Environmental Engineering, Universitas Gadjah Mada, Indonesia.

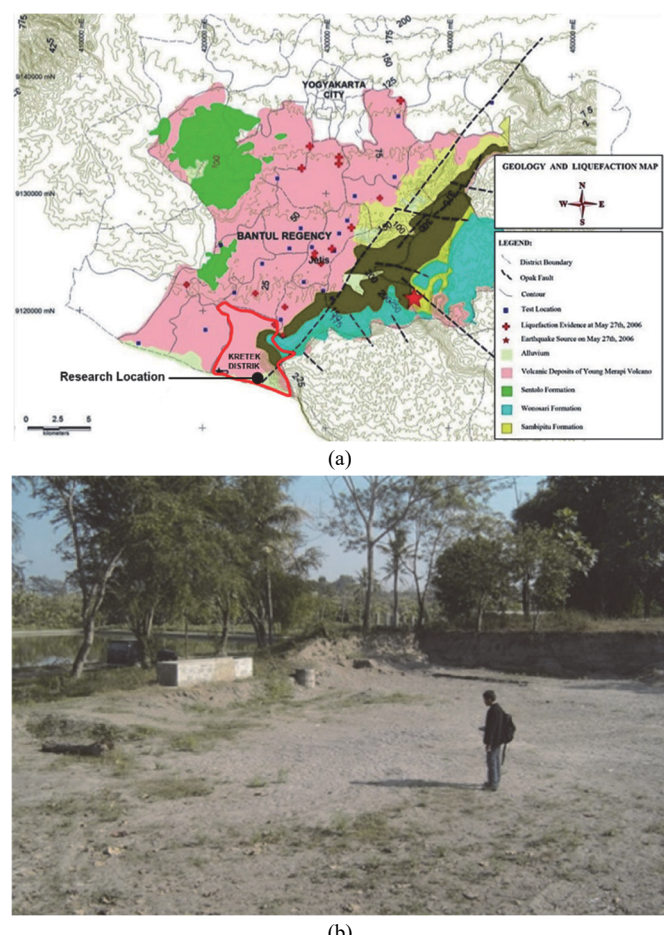


Fig. 1 (a) Identified liquefaction evidence and (b) liquefaction event after the 2006 Bantul earthquake (Buana and Agung 2015)

This research focused on the Kretek 2 Bridge (included in the South Java Line (JLSS)), Kretek district, Bantul Regency, Indonesia. Several studies have shown that the soil in Bantul Regency, particularly near the Opak River, is dominantly in the young Quaternary soil category and features a high liquefaction potential. Patalan village, Jetis district, Bantul Regency, located near the Opak fault area, had various thicknesses of liquefaction ranging from approximately 0.2–5.2 m with layer depths varying from 0.2–12.8 m below the soil surface (Soebowo *et al.* 2009), and Kretek district had a high liquefaction potential (Buana *et al.* 2016). Similar results were obtained by Laia (2015), who studied sandy soil in the Opak River Pleret district by using the shaking table test method, and Mase (2017), who studied sandy soils from the Opak River Imogiri district. Additionally, Rahman *et al.* (2020) showed that the liquefaction potential of the Yogyakarta International Airport Underpass area ranged from low to high. The airport is 28 km from the epicenter of the Bantul earthquake. These facts confirm that liquefaction potential analysis is a prerequisite before developing important structures in Bantul Regency.

2. METHODOLOGY

Determining the peak ground acceleration (PGA) value is the first step in assessing liquefaction potential. Soebowo *et al.* (2009) defined the maximum PGA value in Bantul Regency as 0.487 g. Using the Kanai equation by 231 microtremor data and earthquake events from 1981–2014, Wibowo and Sembri (2016) showed that the maximum PGA in Bantul Regency was 0.421 g. Referring to the Indonesian earthquake source and hazard map (2017), we can estimate the PGA value at bedrock by using probabilistic seismic hazard analysis (PSHA) and deterministic seismic hazard analysis (DSHA) (National Earthquake Study Center 2017). By using the PSHA method (Indonesian National Standardization Agency 2016), this study applied a 7% probability of exceedance in 75 years, equivalent to 1000 years, following the Indonesian National Standard (SNI) 2833-2016. For practical reasons in determining the PGA value with the PSHA method, this study used the LINI web-based application by the Ministry of Public Works and Housing Indonesia (Directorate General of Highways 2021).

In addition to the PGA value at bedrock, the amplification factor for each site is also essential. By SNI 8460-2017, the site class amplification factor (F_{PGA}) can be determined by the average SPT-N (standard penetration test blow count) or average V_{S30} (shear wave velocity to a depth of 30 m) value (Indonesian National Standardization Agency 2017), as shown in Table 1. By using USGS and microtremor data, Wibowo (2017) mapped the V_{S30} value in Bantul Regency. He concluded that the V_{S30} value in Kretek District was approximately 250 to 350 m/s. Based on the field geotechnical report for nine boreholes of SPT-N and two boreholes of V_{S30} from the downhole seismic test, all boreholes were classified as having medium soil (SD), most of which with medium to dense sand. Based on Table 1, $F_{PGA} = 1.0$ was obtained for $PGA \geq 0.5$ g and the medium soil site class category.

Calculating the PGA result using the LINI application in Bantul Regency, the PGA maximum value is 0.558 g. Next, this value had to be multiplied by $F_{PGA} = 1.0$; thus, the PGA value on the surface (PGAM) was 0.558 g. Since the distance between each borehole's location and the Opak fault epicenter was less than 1.0 km, the PGAM value would be applicable for each borehole in determining liquefaction potential.

Table 1 Site class amplification factor for PGA (SNI 8460:2017)

Site Class	SPT-N	V_{S30} (m/s)	PGA (g)				
			≤ 0.1	0.2	0.3	0.4	≥ 0.5
SA (Hard rock)	—	> 1,500	0.8	0.8	0.8	0.8	0.8
SB (Rock)	—	750–1,500	1.0	1.0	1.0	1.0	1.0
SC (Hard soil)	> 50	350–750	1.2	1.2	1.1	1.0	1.0
SD (Medium soil)	15–50	175–350	2.5	1.7	1.2	1.1	1.0
SE (Soft soil)	< 15	< 175	2.5	1.7	1.2	0.9	0.9

2.1 Simplified Procedure for Evaluating Soil Liquefaction Potential

One of the recent approaches to estimating the safety factors against liquefaction is a simplified procedure proposed by Idriss and Boulanger (2008). These researchers determined the safety factor value by calculating the cyclic resistance ratio as a soil countermeasure against cyclic stress on the soil during an earthquake (see Eq. (1)). Furthermore, the cyclic resistance and cyclic stress ratio can be determined by considering the SPT-N determined through soil investigation, soil properties from a laboratory test, and the PGA and moment magnitude of the earthquake determined on-site with the following equation:

$$SF = \frac{CRR}{CSR} \quad (1)$$

$$CSR = 0.65 \frac{a_{\max}}{g} \frac{\sigma_{vc}}{\sigma'_{vc}} \frac{1}{MSF} \frac{1}{K_{\sigma}} r_d \quad (2)$$

$$\begin{aligned} CRR = \exp & \left(\frac{(N_1)_{60cs}}{14.1} + \left(\frac{(N_1)_{60cs}}{126} \right)^2 - \left(\frac{(N_1)_{60cs}}{23.6} \right)^3 \right. \\ & \left. + \left(\frac{(N_1)_{60cs}}{25.4} \right)^4 - 2.8 \right) \end{aligned} \quad (3)$$

where SF is the safety factor against liquefaction, CSR is the cyclic stress ratio, CRR is the cyclic resistance ratio, the 0.65 coefficient represents a value equal to 65% of the peak cyclic stress, a_{\max} is the maximum peak ground acceleration on the surface, g is the effect of gravity on Earth (9.8 m/s²), σ_{vc} and σ'_{vc} are the total and effective vertical stress, MSF is the magnitude scaling factor of the moment magnitude 7.5, K_{σ} is the overburden correction factor, and r_d is the shear stress reduction coefficient that correlates the depth function and magnitude scale. $(N_1)_{60cs}$ refers to SPT-N after correction, which includes effective overburden stress correction (N_1), soil investigation boring equipment correction (N_{60}), and fines content of soil correction (N_{cs}). The occurrence of liquefaction is likely if the safety factor value is less than 1.0.

2.2 Quantitative Indices for Evaluating Liquefaction Potential

Many researchers have studied the quantitative liquefaction potential. This study attempted to compare various methods, namely, the Liquefaction Potential Index (LPI) by Iwasaki *et al.* (1981), Liquefaction Reduction Number (LRN) by Chung and Rogers (2017), Liquefaction Risk Index (LRI) by Lee *et al.* (2003), Liquefaction Severity Index (LSI) by Sonmez and Gokceoglu (2005), Liquefaction Displacement Index (LDI) by Zhang *et al.* (2004), and Post-Liquefaction Settlement by Idriss and Boulanger

(2008). All those methods used the safety factor value obtained from the simplified procedure or other empirical equation-based on-site investigations. Iwasaki *et al.* (1981) proposed the liquefaction potential index method to assess the liquefaction potential factor with the following equation:

$$LPI = \int_0^{20} F \cdot w(z) dz \quad (4)$$

$$F = 1 - SF \quad \text{for } SF < 1$$

$$F = 0 \quad \text{for } SF \geq 1$$

$$w(z) = 10 - 0.5z \quad \text{for } 0 \leq z < 20$$

$$w(z) = 0 \quad \text{for } z \geq 20 \quad (5)$$

where LPI is the liquefaction potential index, F represents a weighting factor for SF (factor of safety), $w(z)$ represents a weighting factor for depth, and z is depth (m). The LPI has a quantitative value from 0 to 100. A qualitative category for the range of liquefaction vulnerability potential is presented in Table 2 below:

Table 2 Liquefaction potential category (Iwasaki *et al.* 1981)

Potential index	Category
LPI = 0	very low
0 < LPI ≤ 5	low
5 < LPI ≤ 15	high
LPI > 15	very high

Chung and Rogers (2017) proposed the Liquefaction Reduction Number (LRN) method to supplement the LPI method based on non-liquefied sites because the non-liquefied sites present higher values than the liquefied sites. In many cases, the LPI can have different liquefaction probabilities with the same values. Therefore, the LRN is needed to calibrate the LPI values. The LRN can be estimated (0-100) with the following equation:

$$LRN = \int_0^{20} R \cdot w(z) dz \quad (6)$$

$$R = 0 \quad \text{for } SF < 1$$

$$R = (SF - 1) / (n - 1) \quad \text{for } 1 \leq SF < n$$

$$R = 1 \quad \text{for } SF \geq n \text{ or non-liquefiable layer}$$

$$w(z) = 10 - 0.5z \quad \text{for } z \leq 20 \text{ m} \quad (7)$$

where R is the reduction factor of liquefaction, $w(z)$ is the weight function of depth (≤ 20 m), z is depth (m), and n is the minimum SF for no expectation of liquefaction occurrence (this study uses $n = 1.2$). The LRN has a qualitative category, as presented in Table 3 below.

Table 3 Liquefaction reduction number categories (Chung and Rogers 2017)

Reduction number	Category
LRN < 70	very high
70 < LRN ≤ 80	high
LRN > 80	low

Other researchers, Lee *et al.* (2003), proposed the liquefaction risk index (LRI) method of updating the LPI. The LPI categorizes a site as having a high liquefaction potential with index values of 5-15. As a result, some sites where no actual liquefaction occurred were identified as having liquefaction potential by the LPI. Therefore, the LPI method needs to be recalibrated using the LRI so that the potential prediction approaches the extent of an actual liquefaction event. The LRI can be determined by using the following equations:

$$LRI = \sum_0^{20} P_L \cdot w(z) dz \quad (8)$$

$$P_L = \frac{1}{1 + (\frac{SF}{0.96})^{4.5}}$$

$$w(z) = 10 - 0.5z \quad (9)$$

where LRI is the liquefaction risk index, P_L is the probability of liquefaction, $w(z)$ is the weight function of depth (≤ 20 m), and z is depth ($z \leq 20$ m). The LRI has a quantitative value from 0 to 100. A qualitative category for the range of liquefaction probability is presented in Table 4 below:

Table 4 Liquefaction risk category (Lee *et al.* 2003)

Risk index	Category
0 < LRI ≤ 20	low
20 < LRI ≤ 30	medium
30 < LRI ≤ 100	high

Sonmez and Gokceoglu (2005) also proposed a liquefaction severity index (LSI) with the same approaches. However, with different limitations of the SF value, SF can still be input into the LSI with a maximum value of 1.411. The following Eqs. (10) and (11) calculate the liquefaction severity index:

$$LSI = \int_0^{20} P_L(z) \cdot w(z) dz \quad (10)$$

$$P_L(z) = \frac{1}{1 + (\frac{SF}{0.96})^{4.5}} \quad \text{for } SF \leq 1.411$$

$$P_L(z) = 0 \quad \text{for } SF > 1.411$$

$$w(z) = 10 - 0.5z \quad (11)$$

where LSI is the liquefaction severity index, $P_L(z)$ is the probability of liquefaction, $w(z)$ is the weight function of depth (≤ 20 m), and z is depth ($z \leq 20$ m). The LSI has a quantitative value from 0 to 100. However, for a qualitative classification of the range of liquefaction probability, the LSI is more specific and divided into six classes. The classification is presented in Table 5.

Table 5 Liquefaction severity classification (Sonmez and Gokceoglu 2005)

Severity index	Class
LSI = 0	non-liquefied
0 < LSI ≤ 15	very low
15 < LSI ≤ 35	low
35 < LSI ≤ 65	moderate
65 < LSI ≤ 85	high
85 < LSI ≤ 100	very high

Different from other previous methods, the liquefaction displacement index (LDI) was proposed by Zhang *et al.* (2004) to estimate lateral displacement induced by liquefaction events by using the standard penetration test (SPT) or cone penetration test (CPT). This empirical method used historical case data from previous earthquakes and induced lateral displacement. LDI comes from the following Eqs. (12) and (13):

$$\text{LDI} = \int_0^{z_{\max}} \gamma_{\max} dz \quad (12)$$

where z_{\max} is the maximum depth of potential liquefaction layers with calculated SF less than 2, γ_{\max} is the maximum amplitude of cyclic shear strain induced during undrained cyclic loading for a saturated sandy soil, and z is depth (m). In this equation, both γ_{\max} and the thickness of liquified soil layers can be affected by soil properties and earthquake magnitude.

$$\begin{aligned} \gamma_{\max} &= 3.26(\text{SF})^{-1.80} && \text{for } 0.7 \leq \text{SF} \leq 2.0 \\ \text{or } \gamma_{\max} &= 6.2 && \text{for } \text{SF} \leq 0.7 [D_r = 90\%] \\ \gamma_{\max} &= 3.22(\text{SF})^{-2.08} && \text{for } 0.56 \leq \text{SF} \leq 2.0 \\ \text{or } \gamma_{\max} &= 10 && \text{for } \text{SF} \leq 0.56 [D_r = 80\%] \\ \gamma_{\max} &= 3.20(\text{SF})^{-2.89} && \text{for } 0.59 \leq \text{SF} \leq 2.0 \\ \text{or } \gamma_{\max} &= 14.5 && \text{for } \text{SF} \leq 0.59 [D_r = 70\%] \\ \gamma_{\max} &= 3.58(\text{SF})^{-4.42} && \text{for } 0.66 \leq \text{SF} \leq 2.0 \\ \text{or } \gamma_{\max} &= 22.7 && \text{for } \text{SF} \leq 0.66 [D_r = 60\%] \\ \gamma_{\max} &= 4.22(\text{SF})^{-6.39} && \text{for } 0.72 \leq \text{SF} \leq 2.0 \\ \text{or } \gamma_{\max} &= 34.1 && \text{for } \text{SF} \leq 0.72 [D_r = 50\%] \\ \gamma_{\max} &= 3.31(\text{SF})^{-7.97} && \text{for } 1.0 \leq \text{SF} \leq 2.0 \\ \text{or } \gamma_{\max} &= 250(1.0 - \text{SF}) + 3.5 && \text{for } 0.81 \leq \text{SF} \leq 1.0 \\ \text{or } \gamma_{\max} &= 51.2 && \text{for } \text{SF} \leq 0.81 [D_r = 40\%] \end{aligned} \quad (13)$$

$$D_r = 14\sqrt{(N_1)_{60}} \quad \text{for } [(N_1)_{60} \leq 42] \quad (14)$$

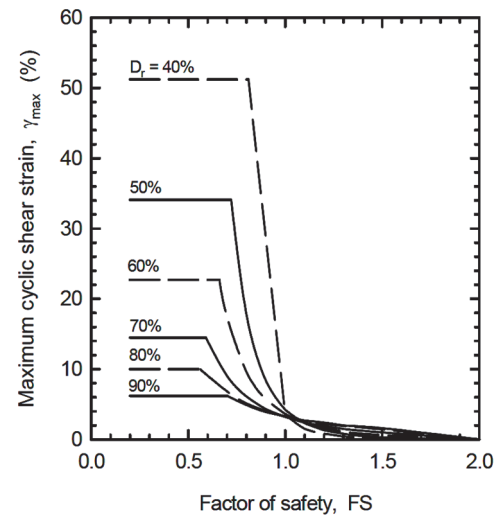
In determining the γ_{\max} equation, the values of the relative density (D_r) and SF must be defined first by referring to the correlation between γ_{\max} and the relative density graph by Ishihara and Yoshimine (1992), as presented in Fig. 2(a). The relative density can be calculated with the correlation (N_1)₆₀ value by using Eq. (14). (N_1)₆₀ is SPT-N corrected by the effective overburden stress and soil boring equipment.

The next step in estimating lateral displacement (LD) involves assuming that the ground slope (S) follows Eq. (15) and/or the free face height (H) follows Eq. (16). LDI is the lateral displacement index, S is the ground slope, and L is the horizontal distance from the toe of a free face.

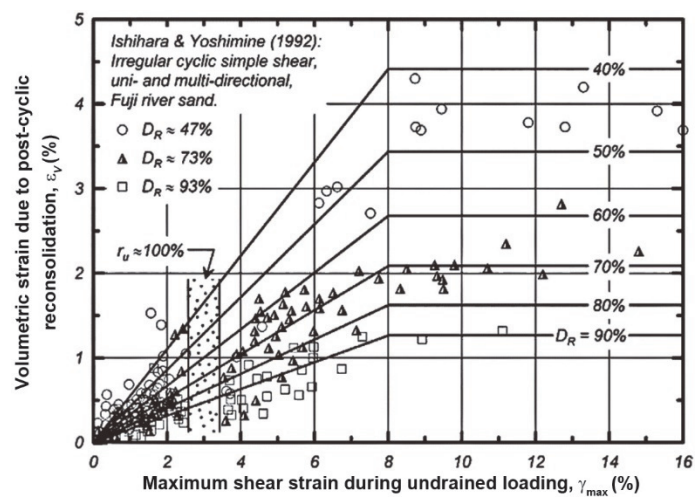
$$LD = (S + 0.2) \text{LDI} \quad \text{for } 0.2\% < S < 3.5\% \quad (15)$$

$$LD = 6\left(\frac{L}{H}\right)^{-0.8} \text{LDI} \quad \text{for } 4 < \frac{L}{H} < 40 \quad (16)$$

Post-liquefaction settlement is another method for determining potential liquefaction by quantitative analysis. Idriss and Boulanger (2008) proposed one-dimensional reconsolidation by calculating vertical strains to volumetric strains and integrating them to the depth interval with the following equation:



(a)



(b)

Fig. 2 (a) Correlations among γ_{\max} , safety factor, and relative density, and (b) Correlations among γ_{\max} , ϵ_v , and relative density (Ishihara and Yoshimine 1992)

$$S_{v-1D} = \int_0^{z_{\max}} \epsilon_v dz \quad (17)$$

$$\epsilon_v = 1.5 \times \exp(-2.5D_R) \times \min(0.08, \gamma_{\max}) \quad \text{or}$$

$$\epsilon_v = 1.5 \times \exp(-0.369\sqrt{(N_1)_{60}}) \times \min(0.08, \gamma_{\max}) \quad (18)$$

where ϵ_v is the volumetric strain due to post-cyclic reconsolidation proposed by Yoshimine *et al.* (2006) and D_R is the relative density, which can be calculated with Eq. (14). γ_{\max} is the maximum shear strain during undrained loading. γ_{\max} is limited by a maximum value of 8% based on the correlation graph among γ_{\max} , ϵ_v , and relative density by Ishihara and Yoshimine (1992), as redrawn in Fig. 2(b).

Although the LPI, LRN, LRI, and LSI have the same variables in determining the level of liquefaction potential based on the safety factor's value, these four indices have differences. The LPI is the method first proposed by Iwasaki *et al.* (1981) based on 64 liquefied sites and 23 non-liquefied sites from 6 earthquake events in Japan. Chung and Rogers (2017) stated that the LPI method

provided overestimated results in some locations; therefore, they proposed the LRN. The data references for the LRN method used 185 liquefied sites and 294 non-liquefied sites. Additionally, Lee *et al.* (2003) researched liquefaction events in Yuanlin, Taiwan, after the 1999 Chi-Chi earthquake by using data from 72 CPTs and then proposed the LRI. This method is suitable for predicting liquefaction cases in the 1999 Chi-Chi earthquake in areas with medium to dense sandy soil characteristics. Sonmez and Gokceoglu (2005) proposed the LSI method because some areas that were considered not prone to liquefaction under the LPI could not be clearly distinguished. The LSI also has more detailed qualitative categories of liquefaction potential with respect to severity.

Based on empirical data from 13 earthquakes, the LDI method aims to obtain the potential of lateral displacement when liquefaction occurs. The empirical data included lateral distribution, laboratory tests, and previous research. However, the accuracy of the resulting values compared to the measured values still had a deviation of approximately 0.1 to 1.92 m. Furthermore, to predict the vertical displacement of soil, the post-liquefaction settlement method was developed based on field observations and previous research on volumetric strain. The assessment of lateral displacement and settlement can affect the foundation design.

3. RESULTS OF THE CASE STUDY

The soil investigation was carried out at the Opak River (see Fig. 3) with nine boreholes (BH-1 to BH-9). The density of the sandy soil used the “very loose” category for SPT-N 0-4, “loose” category for SPT-N 4-10, “medium” category for SPT-N 10-30, “dense” category for SPT-N 30-50, and “very dense” category for SPT-N >50 (Loo, 2007). The investigation findings showed that the soil was dominantly medium-dense sand, except at 1.5-6 m depth at BH-1, BH-2, BH-3, BH-5, BH-6, BH-7, and BH-8, where the soil tended to be loose-medium sand.

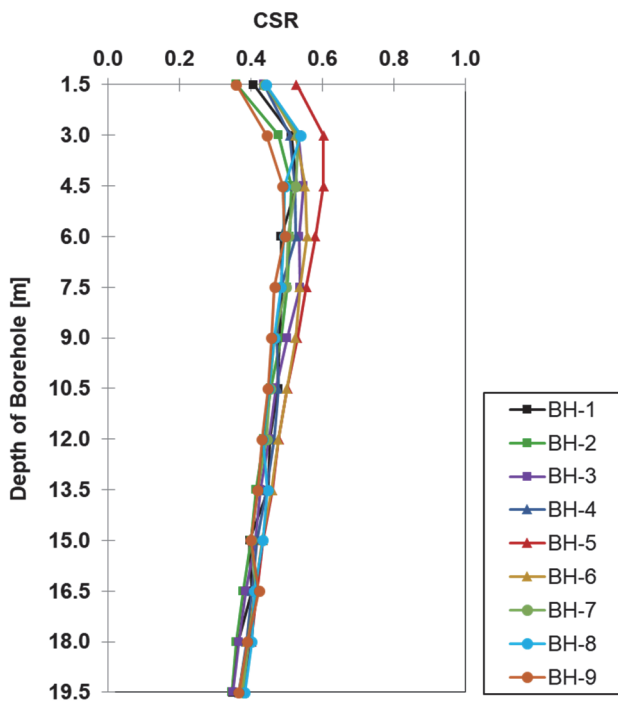


Fig. 4 CSR results for 9 boreholes

3.1 Safety Factor against Liquefaction

The simplified procedure calculation using a PGA of 0.558 g and a moment magnitude of 6.2 resulted in various CSR values from 0.346 to 0.603 and various CRR values from 0.168 to 2.0 (see Figs. 4 and 5). The potential of liquefaction spreads in the loose to medium sand layers at 1.5-6 m depth with a SF value of less than 1.0. Liquefaction potential occurs in the 16.5 m depth layer for all boreholes except BH9 and BH-4 has non-liquefied soil in all soil layers (see Table 6).



Fig. 3 Borehole locations (Google Earth 2023)

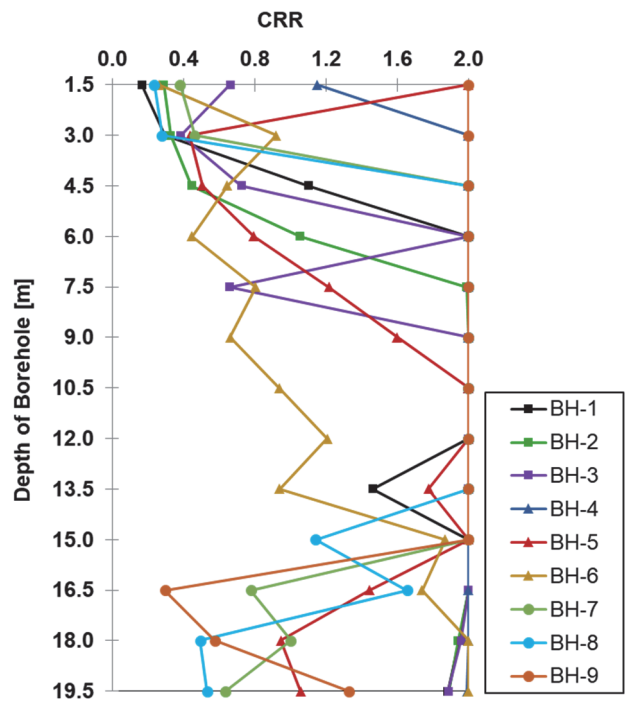


Fig. 5 CRR results for 9 boreholes

Table 6 Safety factor against liquefaction and density of the sandy soil in each layer

SF									
Depth of Borehole [m]	BH-1	BH-2	BH-3	BH-4	BH-5	BH-6	BH-7	BH-8	BH-9
0.0	0.413	0.807	1.522	2.642	3.800	0.600	0.872	0.537	5.585
1.5	0.573	0.688	0.725	3.932	0.725	1.756	0.872	0.519	4.511
3.0	2.094	0.873	1.326	3.829	0.843	1.174	3.818	4.055	4.096
4.5	4.145	2.076	3.738	3.809	1.374	0.805	3.972	4.069	4.053
6.0	4.108	3.973	1.233	4.147	2.199	1.504	4.021	4.147	4.303
7.5	4.180	4.128	4.006	4.242	3.029	1.263	4.287	4.297	4.378
9.0	4.219	4.403	4.263	4.209	3.992	1.877	4.412	4.447	4.475
10.5	4.416	4.582	4.454	4.310	4.190	2.538	4.508	4.621	4.646
12.0	3.269	4.827	4.695	4.518	3.871	2.054	4.790	4.487	4.787
13.5	5.064	4.999	4.870	4.794	4.626	4.343	4.999	2.641	5.013
15.0	4.978	5.314	5.208	4.989	3.466	4.237	1.882	4.057	0.704
16.5	5.377	5.410	5.358	5.174	2.370	5.138	2.556	1.233	1.480
18.0	5.425	5.461	5.405	5.434	2.791	5.380	1.679	1.396	3.644
19.5	SF < 1.0								

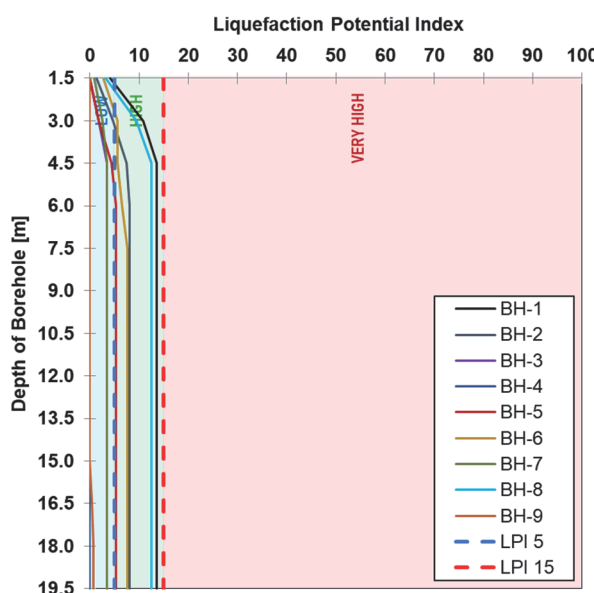


Fig. 6 LPI cumulative value based on depth

3.2 Quantitative Indices of Liquefaction Potential

The quantitative index results of each method are displayed in the cumulative graph. Each change in the shape of the graph with depth indicates an increase in the potential liquefaction value. The result of the cumulative LPI value shows various values from 0 to 13.584, with categories for BH-1, BH-2, BH-5, BH-6, and BH-8 being “high potential”, BH-3, BH-7, and BH-9 being “low potential”, and BH-4 being “very-low potential” or 0 (see Fig. 6). The LRN also shows that the soil features very high to low potentials with values of 54.188 to 92.438. The very high potential category is found in BH-1, BH-2, BH-5, BH-6, BH-7, and BH-8; the “high potential” category is found in BH-3; and the “low potential” category is found in BH-4 and BH-9 (see Fig. 7). The potential liquefaction has results similar to those of the LPI and LRN methods, except for BH-3 and BH-7.

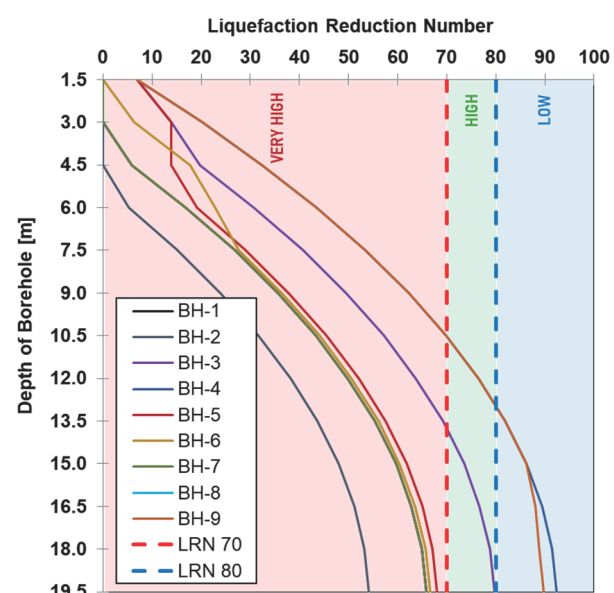


Fig. 7 LRN cumulative value based on depth

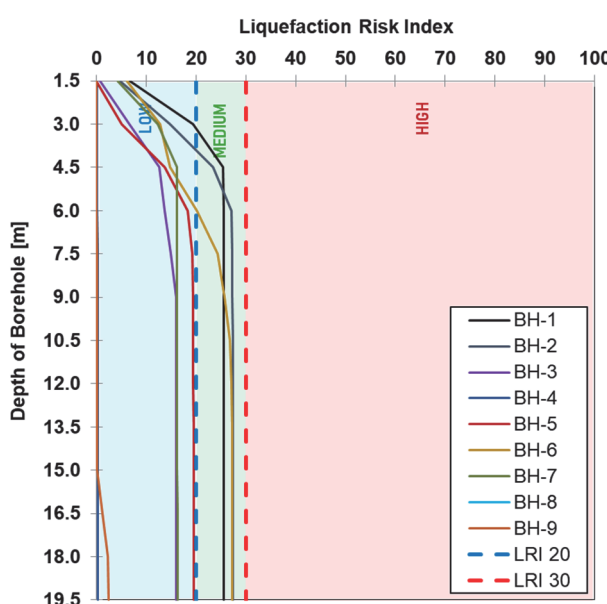


Fig. 8 LRI cumulative value based on depth

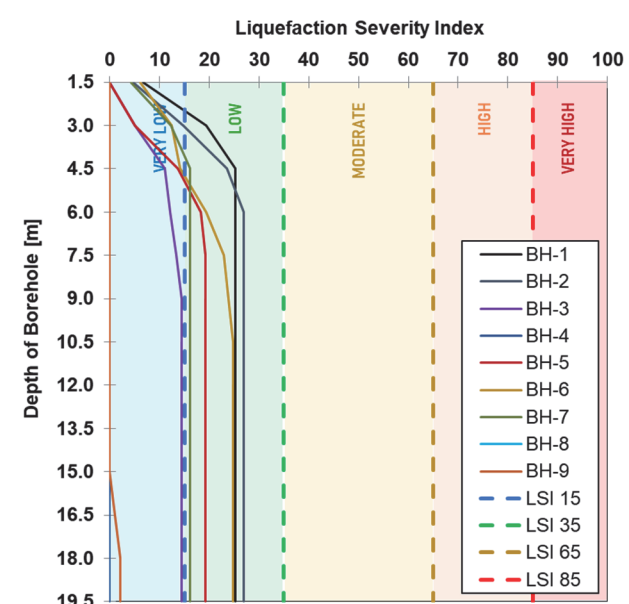


Fig. 9 LSI cumulative value based on depth

The LRI results show that the soil is dominantly categorized into low and medium categories with various values from 0.260 to 27.352. The medium category is observed in BH-1, BH-2, BH-6, and BH-8, and the low category is observed in BH-3, BH-4, BH-5, BH-7, and BH-9 (see Fig. 8). However, the LSI results are slightly different from the LRI results. The soil has a potential classification of very low and low, ranging from 0 to 26.987. The low class is observed in BH-1, BH-2, BH-5, BH-6, BH-7, and BH-8; the very-low class is observed in BH-3 and BH-9; and BH-4 is non-liquefied in all layers (see Fig. 9). Although the LRI and LSI methods have similar equation sources, they have different qualitative categories or classifications. The overall quantitative index results for each borehole are shown in Fig. 10.

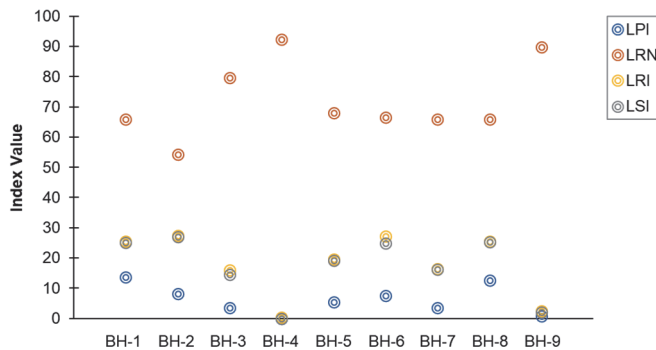


Fig. 10 Quantitative results of each borehole using the LPI, LRN, LRI, and LSI methods

For the LDI method, the lateral displacement results in a maximum value of 3.824 m in BH-1 and a minimum value of 0 m in BH-4 and BH-9. The post-liquefaction settlement results include a maximum value of 0.114 m in BH-1 and a minimum value of 0 m in BH-4. In BH-9 (see Figs. 11 and 12), although settlement potentially occurs, no lateral displacement event due to a liquefaction potential of SF < 1.0 occurs at a depth of 16.5 m.

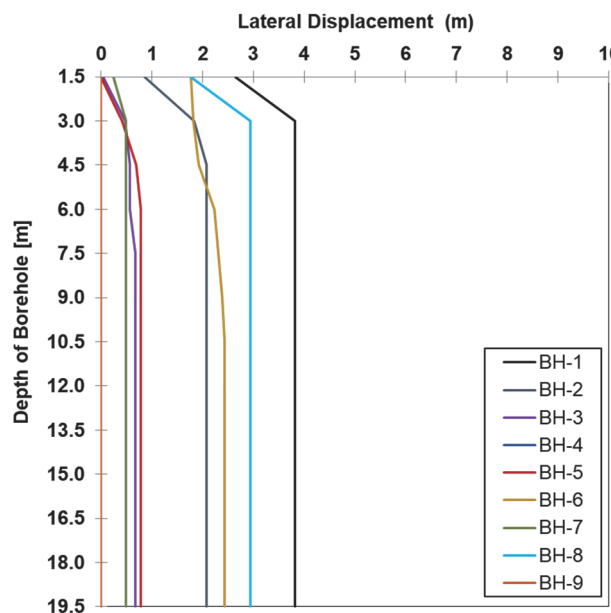


Fig. 11 LDI cumulative value based on depth

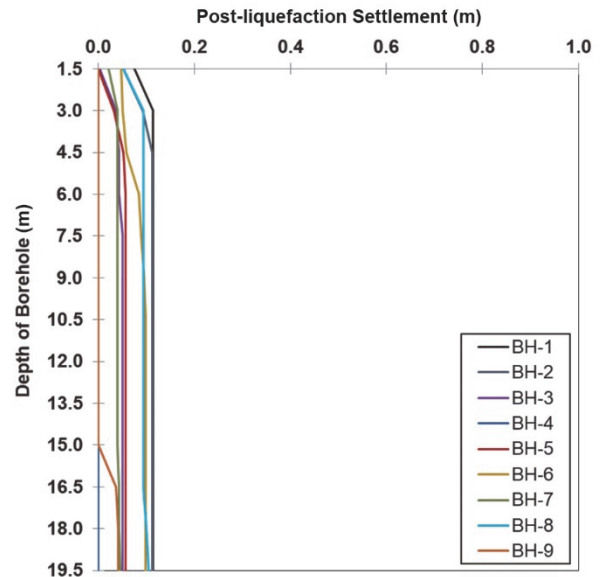


Fig. 12 Post-liquefaction settlement cumulative value based on depth

4. COMPARISONS AND DISCUSSIONS

The results of this study show that in areas with medium-dense sand, liquefaction potential still exists. Liquefaction potential is higher at shallow depths with very loose to medium-dense sand. The liquefaction potential is observed at all borehole locations except BH-4.

4.1 Overall Comparison of Quantitative Indices

For a quantitative analysis, the LPI method is based on Iwaki *et al.* (1981), who showed that soil can be classified into low and high categories for liquefaction potential. However, in the LPI results, there are only two outcomes, low and high potential. This fact indicates that the LPI is suitable for estimating a yes-no likelihood of liquefaction occurrence. If there are any liquefaction layers with a minimum thickness of 3.0 m but that are significantly low, then that soil can have a high liquefaction potential. This situation occurs in BH-1, BH-5, and BH-8. The LRN method calibrates the LPI method by considering non-liquefied sites. The results of this method show that the categories can be more diverse, from "low" to "very high" potentials. However, in BH-3 and BH-7, there are some differences between the LPI and LRN due to different limitations of the SF value in defining the liquefaction state, that is, 1.0 for the LPI and 1.2 for the LRN. For the LRN result, BH-3 falls into the high potential and BH-7 into the very high potential category, while the LPI shows low potential at these boreholes (see Fig. 13).

The LRI and LSI methods aim to update the LPI method by assessing the risk and severity of liquefaction occurrences. Even though the LRI and LSI equations look similar, they are slightly different in terms of the SF value limits. In the LRI, there is no limit to the value of SF, whereas in the LSI, the maximum SF used is less than or equal to 1.411. In addition, the LRI only has three categories for liquefaction potential, but the LSI has six classifications, making it more detailed. Nevertheless, these methods have similar quantitative results (all values are less than 30, unlike those of the LRN) (see Fig. 13).

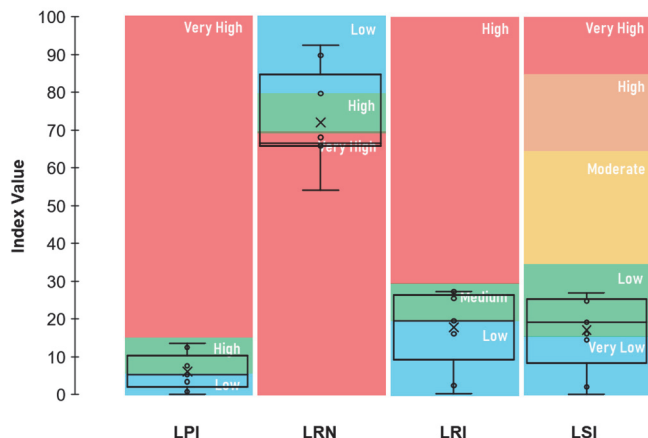


Fig. 13 Comparison results of LPI, LRN, LRI, and LSI methods

The results of the LDI and post-liquefaction settlement methods show that both lateral displacement and settlement have linear increments. The higher the lateral displacement value is, the higher the settlement value at the same borehole. This condition might occur because the equation to estimate lateral displacement and post-liquefaction settlement uses the same maximum cyclic shear strain variable. Except for BH-9, despite a settlement of 0.041 m, there is no lateral displacement at the soil surface caused by liquefaction potentially occurring to a depth of 16.5 m. Even so, referring to Ishihara (1985), if the surface soil layer without liquefaction is thicker than the liquefaction layer below it, it can reduce the impact on the structure.

4.2 Comparison of Quantitative Indices at Different Boreholes

A previous study by Soebowo *et al.* (2009) showed that lateral spreading or sand boiling did not occur in the Opak River estuary after the 2006 Bantul earthquake. The distribution of liquefaction is concentrated in the northern and eastern parts of Bantul Regency and around the Opak River. Nevertheless, the liquefaction potential in the Kretek 2 Bridge area is still present based on the simplified procedure approach with a resulting SF value < 1.0 for almost all boreholes. The LPI and LRN results show that BH-1, BH-2, BH-5, BH-6, and BH-8 had consistent values with high and very high potential, while BH-4 and BH-9 showed equally very low or low potential. In BH-3 and BH-7, there are significant differences in the results. This output shows that the LRN corrects the value generated by the LPI from initially low potential to high or very high potential. These results also confirm that the LRN is a complementary method that can be used together with the LPI for more reliable results. The LSI results have a low to medium risk output, and the LRI shows a very low to low severity index output; furthermore, at BH-4, the results indicated non-liquefaction. The LRI and LSI methods tend to have lower qualitative outputs than the LPI and LRN methods. This is because the LRI and LSI emphasize the impacts of liquefaction in terms of risk and severity, respectively. The LSI tends to have the lowest value. At the same time, the results of the LDI method and post-liquefaction settlement on BH-1, BH-2, BH-6, and BH-8 showed large lateral displacements and settlements. The lateral displacements that occurred were 3.824, 2.078, 2.431, and 2.939 m. In terms of the post-liquefaction settlement, the results were 0.114, 0.112, 0.098, and

0.104 m, respectively. The displacement outputs are in line with the results of the LPI and LRN, indicating that the boreholes have high and very high liquefaction potentials and medium and low yields of the LRI and LSI, respectively. Additionally, BH-4 consistently has dense to very dense soil density in all layers. At BH-4, there is no value of SF < 1.0 in any layer, so the liquefaction potential index values tend to be very low or low, and there is absolutely no lateral displacement and settlement.

However, the LPI can still be used in a study due to the simple category with high to low potential outputs. For calibrating and complementing the LPI method in a location with a dominant non-liquefied layer such as the one in this research, the LRN method can update the LPI method with a more reliable potential liquefaction value. To consider risk probability and depth weighting, the LRI method has three categories (low, medium, and high). However, the LSI method can also be chosen for a more detailed qualitative result. In addition to liquefaction potentials, the LDI and post-liquefaction settlement methods offer only a quantitative model to predict lateral displacement and settlement value due to liquefaction. Thus, all quantitative analyses can be used depending on the research need. A summary of the quantitative analysis of the liquefaction potential in the Kretek 2 Bridge area can be seen in Table 7 below.

Further analysis of the impact of liquefaction on the foundation of the structure can be further investigated at BH-1, BH-2, BH-6, and BH-8. Those boreholes consistently have moderate to very high liquefaction potentials with various methods (only the LSI results are only in the low category). They also exhibit high lateral displacement values of 2.078-3.824 m and settlements of 0.098-0.114 m.

5. CONCLUSIONS

Even though it is in an area with medium to dense sand characteristics, there is a surface layer with a very loose to medium-dense sand. This soil density class is located at a depth of 1.5-6 m, except in BH-9 where it is at a depth of 16.5 m. In that layer, the liquefaction potentials tend to have a low-high possibility of occurrence with a low to medium risk and severity index. Of the nine boreholes in this study, there are eight boreholes with potential for liquefaction and one borehole with no potential for liquefaction. In this location, the quantitative analyses help to determine the potential liquefaction. The area of the Kretek 2 Bridge has a liquefaction potential of "very low" to "high" by the LPI, "low" to "very high" by the LRN, "low" to "medium" risk by the LRI, and "non-liquefied" to "low" severity by the LSI. Additionally, the lateral displacement is estimated to be approximately 0-3.824 m, and the post-liquefaction settlement is approximately 0-0.114 m.

The proposed method is updated/calibrated based on previous methods. The LPI, LRN, LRI, and LSI methods help estimate liquefaction potentials with consideration of depth factors. However, each method has different result characteristics. The LPI and LRN can be complementary. The LRI and LSI have lower qualitative results than the previous methods, so the results tend to be low to medium. This pattern shows that the LPI and LRN are more inclined to the possibility of a liquefaction event occurring, while the LRI and LSI emphasize the level of risk and severity of liquefaction damage. The thicker the liquefaction layer is, the higher the potential damage.

Table 7 Quantitative analysis results of liquefaction potential

Borehole	Safety factor	LPI		LRN		LRI	
BH-1	liquefied	13.584	high	65.813	very high	25.597	medium
BH-2	liquefied	8.143	high	54.188	very high	27.352	medium
BH-3	liquefied	3.509	low	79.688	high	16.051	low
BH-4	non-liquefied	0.000	very low	92.438	low	0.260	low
BH-5	liquefied	5.339	high	68.063	very high	19.521	low
BH-6	liquefied	7.601	high	66.570	very high	27.269	medium
BH-7	liquefied	3.408	low	65.813	very high	16.386	low
BH-8	liquefied	12.548	high	65.813	very high	25.433	medium
BH-9	liquefied	0.777	low	89.813	low	2.379	low
BH-1	liquefied	25.181	low	3.824		0.114	
BH-2	liquefied	26.987	low	2.078		0.112	
BH-3	liquefied	14.440	very low	0.669		0.051	
BH-4	non-liquefied	0.000	non-liquefied	0.000		0.000	
BH-5	liquefied	19.160	low	0.778		0.057	
BH-6	liquefied	24.813	low	2.431		0.098	
BH-7	liquefied	16.148	low	0.492		0.047	
BH-8	liquefied	25.317	low	2.939		0.104	
BH-9	liquefied	2.104	very low	0.000		0.041	

Furthermore, the LDI and post-liquefaction settlement methods help estimate the lateral displacement and post-liquefaction settlement potentials. The thicker the liquefaction layer at the surface, the greater the lateral distribution and settlement values. The last two methods can be used as indicators of area damage measured in meters if liquefaction occurs.

ACKNOWLEDGEMENT

The authors would like to thank Unit Work of National Road Implementation (PjN) Yogyakarta Special Region Province Territory, National Road Implementation Agency (BBPjN) of Central Java—Yogyakarta Special Region for the soil investigation data support.

FUNDING

This study was supported by a fully funded scholarship in collaboration with The Ministry of Public Works and Housing, Indonesia (MoU no. 16/PKS/M/2016) and Universitas Gadjah Mada, Indonesia (MoU no. 1310/P/Dir-KA/2016).

DATA AVAILABILITY

The data and/or computer codes used/generated in this study are available from the corresponding author on reasonable request.

CONFLICT OF INTEREST STATEMENT

The authors declare that there is no conflict of interest.

REFERENCES

Buana, T.W. and Agung, M.W. (2015). "Liquefaction characteristic based on ground response linear equivalent

analysis and cyclic stress concept on young merapi volcanic deposit in bantul." *10th Asian Regional Conference of IAEG 2015*, 1-5.

https://www.jseg.or.jp/2015ARC/data/TP2/Tp2-10_1072033_1532599.pdf

Buana, T.W., Wafid, M., and Sadisun, I.A. (2016). "Hubungan potensi likuifaksi pada endapan gunungapi merapi muda dengan kerusakan bangunan di kabupaten bantul pada kasus gempabumi 27 Mei 2006." *Journal of Environment and Geological Hazards*, 7(2), 103-111 (in Bahasa). <http://dx.doi.org/10.34126/jlbg.v7i2.98>

Chung, J. and Rogers, J.D. (2017). "Deterministic and probabilistic assessment of liquefaction hazards using the liquefaction potential index and liquefaction reduction number." *Journal of Geotechnical and Geoenvironmental Engineering*, ASCE, 143(10), 04017073. [https://doi.org/10.1061/\(asce\)gt.1943-5606.0001772](https://doi.org/10.1061/(asce)gt.1943-5606.0001772)

Direktorat General of Highways (2021). *Aplikasi LINI Binamarga* (in Bahasa). <http://lini.binamarga.pu.go.id/>

Google Earth (2023). *Citra Satelit Google Earth—Titik Bor Penyelidikan Tanah Jembatan Kretek 2* (in Bahasa). <https://earth.google.com/web/>

Idriss, I.M. and Boulanger, R.W. (2008). "Soil liquefaction during earthquakes." *Machinery and Production Engineering*, Earthquake Engineering Research Institute, 160, 43. <https://doi.org/10.1177/136218079700300202>

Indonesian National Standardization Agency (2016). SNI 2833: 2016 Perencanaan Jembatan Terhadap Beban Gempa, Vol. 2833 (in Bahasa).

Indonesian National Standardization Agency (2017). SNI 8460: 2017 Persyaratan Perancangan Geoteknik, Vol. 8460 (in Bahasa).

Ishihara, K. (1985). "Stability of natural deposits during earthquakes." *Proceedings of 11th International Conference on Soil Mechanics and Foundation Engineering*, San Francisco, 1, 321-376 (Balkema).

- https://www.issmge.org/uploads/publications/1/34/1985_01_0007.pdf
- Ishihara, K. and Yoshimine, M. (1992). "Evaluation of settlements in sand deposits following liquefaction during earthquakes." *Soils and Foundations*, **32**(1), 178-188.
<https://doi.org/10.3208/sandf1972.32.173>
- Iwasaki, T., Tokida, K., and Tatsuoka, F. (1981). "Soil liquefaction potential evaluation with use of the simplified procedure." *International Conferences on Recent Advances in Geotechnical Earthquake Engineering and Soil Dynamics*, **12**, 209-214.
https://scholarsmine.mst.edu/icrageesd/01icrageesd/session0_2/12
- Laia, B. (2015). "The effect of soil density of kali opak pleret yogyakarta sand on liquefaction potential based on." *Jurnal Inersia*, **VII**(1) (in Bahasa).
<http://dx.doi.org/10.46964/inersia.v7i1.541>
- Lee, D.H., Ku, C.S., and Yuan, H. (2003). "A study of the liquefaction risk potential at yuanlin, Taiwan." *Engineering Geology*, **71**(1-2), 97-117.
[https://doi.org/10.1016/S0013-7952\(03\)00128-5](https://doi.org/10.1016/S0013-7952(03)00128-5)
- Look, B.G. (2007). *Handbook of Geotechnical Investigation and Design Tables*, **4**(1), Taylor & Francis Group.
- Mase, L.Z. (2017). "Experimental liquefaction study of southern Yogyakarta using shaking table." *Jurnal Teknik Sipil ITB*, **24**(1), 11-18. <https://doi.org/10.5614/jts.2017.24.1.2>
- National Earthquake Study Center (2017). *Peta sumber dan bahaya gempa indonesia tahun 2017*, Kementerian Pekerjaan Umum dan Perumahan Rakyat (in Bahasa).
https://vsi.esdm.go.id/index.php/kegiatan-pvmbg/download-center/doc_download/5069-peta-sumber-dan-bahaya-gempa-indonesia-tahun-2017
- Nurbaiti, Y., Ibrahim, E., Hasanah, M.U., and Wijatmoko, B. (2019). "Application of double-difference method for relocating aftershocks hypocenters in Opak Fault Zone." *IOP Conference Series: Earth and Environmental Science*, **311**(1), 012028.
<https://doi.org/10.1088/1755-1315/311/1/012028>
- Rahardjo, W., Sukandarrumidi, and Rosidi, H.M.D. (1977). *Geologic Map of the Yogyakarta Quadrangle, Java*, Direktorat Geologi, Departemen Pertambangan, Republik Indonesia.
- Rahman, M.A., Fathani, T.F., Rifa'i, A., and Hidayat, M.S. (2020). "Analisis tingkat potensi likuifaksi di kawasan underpass yogyakarta international airport." *Jurnal Rekayasa Sipil (JRS-Unand)*, **16**(2), 91 (in Bahasa).
<https://doi.org/10.25077/jrs.16.2.91-104.2020>
- Soebowo, E., Tohari, A., and Sarah, D. (2009). "Potensi likuifaksi akibat gempabumi berdasarkan data CPT dan N-SPT di daerah patalan bantul, yogyakarta." *Jurnal RISET Geologi Dan Pertambangan*, **19**(2), 85 (in Bahasa).
<https://doi.org/10.14203/risetgeotam2009.v19.25>
- Sonmez, H. and Gokceoglu, C. (2005). "A liquefaction severity index suggested for engineering practice." *Environmental Geology*, **48**(1), 81-91.
<https://doi.org/10.1007/s00254-005-1263-9>
- Supartoyo, Surono, and Putranto, E.T. (2014). *Katalog gempabumi merusak di inzindonesia tahun 1612-2014*. 5th Ed., Badan Geologi, Kementerian ESDM (in Bahasa).
https://vsi.esdm.go.id/index.php/kegiatan-pvmbg/download-center/doc_download/5074-katalog-gempabumi-merusak-di-indonesia-tahun-1612--2014
- Wibowo, N.B. (2017). "Ratio of Vs30 model based on microtremor and USGS data in jetis bantul." *J. Sains Dasar*, **6**(1), 49-56 (in Bahasa).
<http://dx.doi.org/10.21831/jsd.v6i1.14030>
- Wibowo, N.B. and Sembri, J.N. (2016). "Analisis peak ground acceleration (PGA) dan intensitas gempabumi berdasarkan data gempabumi terasa tahun 1981-2014 di kabupaten bantul yogyakarta." *Indonesian Journal of Applied Physics*, **6**(01), 65 (in Bahasa). <https://doi.org/10.13057/ijap.v6i01.1804>
- Wibowo, N.B. and Sembri, J.N. (2017). "Analysis of seismicity and earthquake energy at opak oyo fault—Yogyakarta." *Indonesian Journal of Applied Physics*, **7**(2), 82 (in Bahasa).
<https://doi.org/10.13057/ijap.v7i2.13702>
- Yoshimine, M., Nishizaki, H., Amano, K., and Hosono, Y. (2006). "Flow deformation of liquefied sand under constant shear load and its application to analysis of flow slide of infinite slope." *Soil Dynamics and Earthquake Engineering*, **26**(2), 253-264.
<https://doi.org/10.1016/j.soildyn.2005.02.016>
- Youd, T.L. and Perkins, D.M. (1978). "Mapping liquefaction-induced ground failure potential." *ASCE Journal of the Geotechnical Engineering Division*, **104**(4), 433-446.
<https://doi.org/10.1061/ajgeb6.0000612>
- Zhang, G., Robertson, P.K., and Brachman, R.W.I. (2004). "Estimating liquefaction-induced lateral displacements using the standard penetration test or cone penetration test." *Journal of Geotechnical and Geoenvironmental Engineering*, ASCE, **130**(8), 861-871.
[https://doi.org/10.1061/\(asce\)1090-0241\(2004\)130:8\(861\)](https://doi.org/10.1061/(asce)1090-0241(2004)130:8(861)